Tutor/s

Dr. Mercè Deumal i Solé
Departament de Ciència de Materials i Química Física

Treball Final de Grau

Triggering the Sign of Magnetic Exchange Coupling in BTBN-based compounds by means of the spin polarisation mechanism.

Activació del Signe de l'Acoblament Magnètic en compostos basats en BTBN mitjançant el mecanisme de polarització d'spin.

Pau Franquesa Viñas

January, 2023

Aquesta obra esta subjecta a la llicència de:
Reconeixement–NoComercial-SenseObraDerivada

http://creativecommons.org/licenses/by-nc-nd/3.0/es/

We are like butterflies who flutter for a day and
think it is forever.

Carl Sagan

A la Mercè per el feedback mostrat des del moment 0, per la paciència i per les nombroses "iteracions"; i a la meva família, perquè malgrat tot el passat ho haurem aconseguit.

REPORT

IDENTIFICATION AND REFLECTION ON THE SUSTAINABLE DEVELOPMENT GOALS (SDG)

This work carries out a systematic theoretical study of different molecules proposed to become suitable candidates for new molecule-based magnets, useful for developing new, better and/or cheaper spintronics devices. These devices show a big capacity in data storage and potential uses on quantum computers. Multiple units and molecules analysed show an enhanced intramolecular ferromagnetic coupling in respect to the BTBN molecule, which is considered as reference. The aim of this work is to contribute with new building blocks to other interested researchers for further investigation into the crystalline structure and its intermolecular magnetic interactions. If adequate candidates are obtained, experimental work could be also carried out and eventually reach a useful material.

Keeping in mind the aim of this work, it can be directly related to the SDG number 9 treating prosperity for the 2030 Agenda. With time passing, more power can be achieved by quantum computers and, thus, this could be largely related to most of the other SDG, since the knowledge learnt could be applied to other areas, such as SDG 13 ("Climate action, researching on slowing down climate change") or SDG 3 ("Good health and well-being researching on new medicines or decreasing the bacterial resistance"), among others.

CONTENTS

1. SUMMARY

‘Spintronic’ devices are based on the spin-polarised electronic currents, taking profit from the intrinsic spin orientation. They are used in traditional knowledge areas such electronics, as well as in other fields of highly potential growing interest, such as quantum computing or neuromorphism. An interesting set of crystalline structures in mixed valance state for these applications are molecule-based magnets, which are usually formed by radical structures showing high spin polarisation regions. The BTBN molecule is used as a reference throughout this TFG in order to design isolated molecules intending an enhanced magnetic-exchange coupling than BTBN, considering modifications on its own basic functional units (A acceptor, C coupler or D donor), aiming at radicals to connect *via* the spin polarisation mechanism. The energetic study for the different spin multiplicity states, carried out using computational methods based on the Densiy Functional Theory (DFT) at a UB3LYP+6-311G(d,p) level for each proposal, is subsequently related to the value of the magnetic coupling J. Broken symmetry (BS) formalism is used in order to provide an adequate diradical description of the singlet open-shell electronic states. The performed study indicates that the called A4 radical unit derived from tetrahiafulvalene in the PA4C1D1 proposal, as a new building block candidate for the design of these organic molecule-based magnets and possible magnetoresistance due to the structural similarities with the TTF. The designed molecule PE1 using an ethylene group with an hydroxyl as C couplers is the one presenting a higher increment in the ferromagnetic exchange coupling J with respect to BTBN

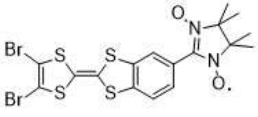

BTBN molecule (A1C1D1)

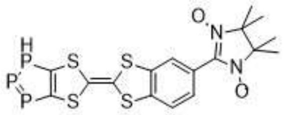

proposal PA4C1D1

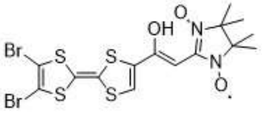

proposal PE1

Keywords: Spin polarization, magnetorresistance, molecular-based magnet, BTBN, magnetic-exchange coupling.

2. RESUM

Els dispositius spintrònics es basen en el flux d'electrons spin polaritzats, és a dir, aprofiten l'orientació dels spins. S'utilitzen tant en camps tradicionals com l'electrònica com en d'altres d'interès creixent com la computació quàntica o neuromòrfica. Un conjunt d'estructures cristal·lines de valència mixta interessants per aquestes aplicacions són els ferroimants orgànics moleculars, sovint formats per estructures radicalàries amb regions d'elevada polarització d'spin, que poden presentar magnetoresistència. La molècula de BTBN s'utilitza com a referència en aquest TFG per dissenyar molècules aïllades procurant que presentin un major acoblament magnètic que el BTBN, considerant modificacions en les unitats bàsiques funcionals (A acceptor, C acoblador , D donador) d'aquest, i buscant que els radicals s'acoblin a través del mecanisme de polarització de spin. L'estudi energètic per als diferents estats de multiplicitat d'spin, fent servir mètodes computacionals basats en la Teoria del Funcional de la Densitat (DFT) a nivell UB3LYP/6-311G+(d,p) per cada proposta, és posteriorment relacionat amb el valor de l'acoblament magnètic J. El formalisme de broken symmetry (BS) s'utilitza per tal de fer una descripció diradicalària adequada dels estats electrònics singlet de capa oberta. L'estudi realitzat senyala a la unitat radicalària derivada del tetratiofulvalè, anomenada A4 a la proposta PA4C1D1, com a nou "building block" candidat per al disseny d'aquests imants orgànics moleculars, i possible magnetoresistència degut a les similituds amb el TTF. La molècula dissenyada PE1, que utilitza grups etilè i hidroxil com a acoblador C és, d'entre les trobades, la que presenta un major increment en l'acoblament J respecte al BTBN.

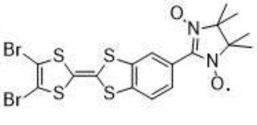
molècula BTBN (A1C1D1)

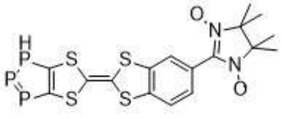
proposta PA4C1D1

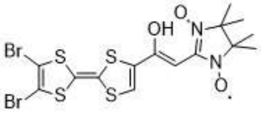
proposta PE1

Paraules clau: polarització de spin, magnetoresistència, ferroimant orgànic molecular, BTBN, acoblament magnètic

3. INTRODUCTION

Magnets have been widely used throughout the history of humanity. Over time, a large quantity of studies provided a wide knowledge about magnetism. Nowadays, it is known to result from cooperative effects between spin carriers with uncompensated spin angular orbital momentum, *i.e.* between radicals.

Commonly, magnets have been based in inorganic structures, such as metals. It was not until 1991 when *Kinoshita and co-workers* [1] showed the world that magnetism could be also observed in purely organic-based structures, known as organic molecular magnets. Apart from being a notorious novelty in magnetism, other interesting abilities such as optical properties, electronic phase transition in solid state or biocompatibility provided them with high potentiality.

These molecular structures are designed by bonding two radical units, whose SOMO (Singly Occupied Molecular Orbital) acts as a magnetic orbital. Magnetic interaction between SOMO's leads to Ferro- or Antiferromagnetic (FM-AFM) J_{AB} coupling when the spins of those electrons align parallel or antiparallel, respectively. This J_{AB} coupling is given when there is an interaction existing between the magnetic spinorbitals in each open-shell unit. These radical moieties can be structures having intrinsically unpaired spins due to an odd electron number (such as nitronyl nitroxide, NN, derivatives). Closed-shell structures, which have experienced charge transfer (oxidation/reduction) phenomena to become radicals with an unpaired electron (*e.g.* tetrahiafulvalene TTF), are also valid magnetic spin units to consider as building blocks. In addition to magnetism, which is enhanced by charge localisation, the spin-carrying centres may undergo charge transport, which would assist conductivity. The presence of both magnetism and conductivity would yield to multifunctional materials, whose potentiality has been acknowledged in the field of spintronics.

In 2006, the magnetoresistance phenomenon was firstly described in a study carried out by *Sugawara, Matushita et al* [2a]. It consisted in an alteration of the magnetic coupling in certain structures when magnetic fields were applied under certain conditions. Henceforth, it became almost a requirement for spintronic applications. This study was focused on TTF (Fig. 1a), a carbon-based structure that, when oxidized, turns into a bicyclic resonant cation radical (Fig. 1b), which acts as magnetic centre, and is responsible of the magnetoresistance properties shown in TTF [2a, 2b].

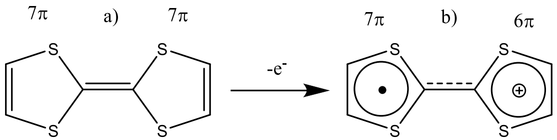

Fig. 1: Tetrathiafulvalene (TTF) monoelectronic oxidation a) TTF structure b) $TTF^{+\bullet}$ structure

On more recent years, further research in the design of organic molecular magnets aiming at new structures with enhanced ferromagnetic response has been carried out [5] . The objective is to provide the interested community with more possible radicals as building blocks and information on the solid-state chemistry. Despite all the exceedingly important information supplied by the crystal packing of these new building blocks (namely, intermolecular coupling interactions and their magnetic topology), this TFG will only focus on the data that can be extracted from the single building block itself.

For the case considered in this work, the discrete BTBN molecule (Fig. 2) is chosen as the reference structure. It consists of one $TTF^{+\bullet}$ unit (acting as magnetic radical centre, A) and a nitronyl-nitroxide radical (NN) (acting as donor radical, D) linked by a phenyl coupler group (C). BTBN, just as TTF unit does, is one of those known molecular organic magnetoresistance coumpounds. In Fig. 2, neutral NN radical acts as a source (D) of specific spin electronic density, which is received by $TTF^{+\bullet}$ radical, working out well for its active magnetic properties (A). Both radicals are linked by a phenyl group, which enables through-bond electronic interactions between radicals.

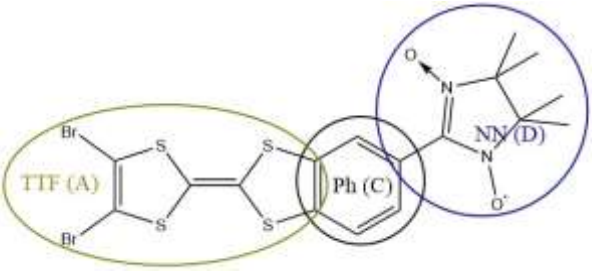

Fig. 2: BTBN molecule (from dibrominated benzo-TTF core and NN).

Computational chemistry tools will be used to design structures similar to BTBN. Indeed, theoretical energy calculations for the discrete considered molecules will be done, as well as geometry optimisations. Data collected from calculations will be used in order to compare these different BTBN-inspired proposed structures in terms of J magnetic coupling to suggest better diradical building blocks with enhanced intramolecular magnetic interaction for possible spintronic applications.

4. OBJECTIVES

Being BTBN the reference structure, the goal of this TFG is to design new similar molecules with stronger magnetic coupling between radicals, enhancing its capacities in magnetism-related phenomena (such as the desired magnetoresistance). This study will only consider intramolecular magnetic interactions between radicals at a discrete level. In the following the specific objectives of this TFG will be outlined.

- The nature of the computational studies carried out demands the use of some programs extensively employed in the area. Note that a large choice of possible methods and codes are available, each one of them with different accuracy level in results. In this TFG, Gaussian has been used for geometry optimisations and energy calculations and Chemcraft for visualisation purposes. Therefore, the first objective is to familiarise with these programs, being capable to do geometry optimisations or frequency calculations. To achieve a good agreement between computational cost and accuracy, the chosen calculation level is based on DFT (Density Functional Theory).
- An initial energy study of BTBN is required to understand its uncommon magnetic properties. TTF and NN building blocks will be independently studied, as well as finally cooperating in BTBN. The objective is to compute the coupling in BTBN (J_{BTBN}) and identify the possible causes for the properties seen.
- Learn how the relation between energies resulting from different total spin multiplicity electronic states for the same structure can be related to a given J_{AB} magnetic coupling between A and B radical units
- Study the influence of some organic groups, when being added or replaced in organic molecule-based magnets, on the resulting electronic structure and its derived

intramolecular properties. It is wanted to be able to distinguish the best groups favouring FM J_{AB} values.

- The main objective, once understood the magnetism in BTBN, is to design (changing/adding/erasing atoms/radicals or other functional groups) different molecules treated as proposals. Further computational studies will assess their magnetic behaviour (FM or AFM). Successful proposals will be the ones which present an enhanced $J_{proposal}$ such that $J_{proposal} > J_{BTBN}$, meaning that ferromagnetism in that specific proposal is larger than in BTBN. This could lead to new diradical ferromagnetic organic magnets containing a TTF or TTF-based unit, being a great candidate to present magnetoresistance too.
- If this improvement is achieved, those new building blocks or structures can be used by experimentalists to tailor new materials for better/cheaper spintronics devices.

5. THEORETICAL BACKGROUND

5.1. FROM QUANTUM MECHANICS TO COMPUTATIONAL CHEMISTRY

Quantum chemistry consists in the atomic-scale study of chemical structures using quantum mechanics theories. Energy calculations play a crucial role, and are given by the famous Schrödinger non time-dependent equation (Eq. 1) formulated in 1926. The Hamiltonian operator $\hat{H}$, when applied to a wavefunction φ (expressed as a sum of a set of $\hat{H}$ eigenfunctions) describing a system, results in energy (E) as the resulting eigenvalue. All nuclear and electronic coordinates are included in φ. Multiple expressions can be derived for $\hat{H}$ depending on the considered contributions to the total energy value given by $\hat{H}$; its fragmentation in contributions from different particles interacting in molecules is shown in Eq. 2.

Eq. 1 $$\hat{H}\varphi = E\varphi$$

Eq. 2 $$\left(\hat{T}_N + \hat{T}_e + \hat{V}_{NN} + \hat{V}_{Ne} + \hat{V}_{ee}\right)\varphi = E\varphi$$

The Born-Oppenheimer (BO) approximation simplifies Eq. 2 separating the motion of nuclei and electrons. Thus, $\hat{H}_{el} = \hat{T}_e + \hat{V}_{Ne} + \hat{V}_{ee}$. Following the BO approach, the idea is to solve the electronic equation shown in Eq. 3 for a fixed nuclei R_I geometry (parametric dependence between solutions found and chosen nuclear coordinates). With the solution obtained, the total energy on nuclear equation (Eq. 4) can be expressed in terms of the Potential Energy Surface (PES) expressed as $U(R_I)$. PES is the overall potential energy, coming from an attractive E_{el} term and a V_{NN} repulsive potential, as shown in Eq. 5

Eq. 3 Schrödinger electronic equation: $\widehat{H}_{el,\,R_I}\ \varphi_{el}(r_i;R_i)=E_{el}(R_I)\varphi_{el}(r_i;R_i)$

Eq. 4 Schrödinger nuclear equation: $\widehat{H}_N\ \varphi_N(R_i)=E\varphi_N(R_i)$

Eq. 5 $\widehat{H}_N=\widehat{T}_N+\widehat{V}_{NN}+E_{el}(R_I)=\widehat{T}_N+U(R_I)$

Hartree and Fock (HF) proposed the Self Consistent Field (SCF) method to solve the electronic Schrödinger equation if a single Slater determinant is considered (monodeterminantal method). Complex expressions in the formulae for SCF methods in addition to their iterative nature result in mathematic expressions difficult to solve even in molecules with a few number of atoms/electrons. The more complex the system is, the more calculation effort is required. SCF solving in HF is the simplest method to an approximation for energy calculations, being truly mathematically complex at the same time. Technological progress since early 30's, when SCF was deduced, has provided us with powerful computers. The use of computation for treating these big amounts of data and difficult calculations to solve complex chemical problems, based in results from quantum mechanics, is known as Computational Chemistry. Computing has thus allowed describing new methods and equations corresponding to more real descriptions for a given system under study.

Multiple computational methods have been developed to introduce, more easily, corrections to the HF method. Different factors can be contemplated in those corrections, and the modified equations become more complex increasing CPU cost when being solved.

5.1.1. HF related methods

By the way HF methods are described, each electron is independent from the others, making correlation energy between electrons (E_{corr}) neglected, and its energy calculated results differ from the exact energy values. Post-HF methods correct this disadvantage by adding this electronic correlation effect:

- Moller-Plesset (MP) approximation introduces E_{corr} as a result of adding a perturbation term in the Hamiltonian. Perturbation is defined as the difference between inter-electronic repulsion and mean effective repulsion, and its first contribution correction results from the 2nd order perturbation.

- Slater determinants are possible electronic configurations for a given chemical agent. Monodeterminantal methods such as HF only consider one electronic configuration in its calculations, normally corresponding to the ground states. Configuration Interaction (CI) approaches E_{corr} describing the wavefunction as a linear combination of different Slater determinants. The use of multiconfigurational wavefunction means that more calculation is needed and better the result is.

The idea applied in the above previous methods is simple: if maths solving is done by a computer, by introducing more strict mathematical equations, reality can be better described. The addition of more terms with different expressions rises CPU cost exponentially. Furthermore, basis functions must be chosen sensibly for an optimal treatment, increasing even more this cost.

5.1.2. Density Functional Theory (DFT)

DFT methods are conceptually different from post-HF methods briefly explained in the section 5.1.1. Before DFT, the external potential $\hat{V}_{Ne}$ in the Hamiltonian operator determines the expressions of the different eigenstates ψ_i for the Hamiltonian. Having the electronic ground eigenstate ψ_0, the electronic density associated to this ground state ρ_0 can be estimated. This procedure is shown in Scheme. 1a for a number m of eigenstates in the system

In DFT, instead of the addition of functions, the observable mono-electronic density $\rho(\vec{r})$ is preferred to correct the missing electronic correlation energy. DFT considers ρ_0 effect on the external potential, resizing the Hamiltonian's expression. Then, it is used to solve the different eigenstates (see Scheme. 1b)

$\hat{V}_{Ne} \rightarrow \psi_i \rightarrow \psi_0, \ldots, \psi_m \rightarrow (\rho_0, E_0), \ldots, (\rho_m, E_m)$

(a): Electronic density is a physical property which can be observed for a certain wavefunction

$\rho_0 \rightarrow \hat{V}_{Ne} \rightarrow \{(\psi_i, E_i)\} = \{(\psi_0, E_0), \ldots, (\psi_m, E_m)\}$

(b): Electronic states expressions derive from electronic densities using functionals.

Scheme1: Comparison between general procedures in(a) HF-related methods, and (b) DFT

DFT theoretical roots were established by Hohenberg-Kohn [3] (HK) theorems announced in 1964. On their 1st, HK stated that given a non-degenerated stationary state ground state, any observable could be calculated if both conditions detailed next are fulfilled. Ground state electronic density function $\rho_0(\vec{r})$ cannot result as the influence of multiple external potentials, only one function (except constants differing) can describe it. Conditions on electronic density were applied in order to do so. On one hand, negative densities make no physical sense, and positive ones are restricted such that $\int \rho(\vec{r})d\vec{r}=n$, where n represents the total number of electrons to ensure an appropriate electronic description for the given system On the other hand, $\rho(\vec{r})$ must be able to be derived from an external potential $\hat{V}_{Ne}$, assuring also a correct representation for this potential effect on the electronic density. This $\rho(\vec{r})$ is defined as seen in Eq. 6, where no spin contributions are considered for the rest of electron; then, the ground state energy can be expressed as a functional of this ground state's density for both cases, shown in Eq. 7.

Eq. 6 $$\rho(\vec{r})=n \int_{\omega_i}\int_{\vec{r}}\dots\int_{\vec{r}_n}|\psi\,(\vec{r},\omega,\,\dots,\,\vec{r}_n)|^2\partial\omega_i\partial\vec{r}\dots\partial\vec{r}_n$$

Eq. 7 $$E[\rho_0(\vec{r})]=F[\rho_0(\vec{r})]+\int_{\vec{r}}\rho_0(\vec{r})\,\hat{V}_{Ne}(\vec{r})\partial(\vec{r})$$

On the 2nd theorem a relationship between $\hat{V}_{Ne}$ and the electronic density of the ground state is established, as seen in Eq. 8. This Variational Principle sketches out the fact that minimizing the density, its expression for the ground state is given, thus E_0 value can be calculated (Eq. 9).

Eq. 8 $$\hat{V}_{Ne}(\vec{r})=-(\delta F[\rho]/\partial\rho)_{\rho=\rho_0}$$

Eq. 9 $$E_0=\min_\rho E[\rho]=E[\rho_0]\leq E[\rho]$$

$F[\rho]$ expression on both Eq. 7 and Eq. 8 refers to an universal functional, common to any electronic system. Approximations are needed because it has no clear mathematical formulations. General expression (Eq. 10), results from kinetic energy T and inter-electronic potential V_{ee}. Note that V_{ee} depends on a classical $J[\rho]$ (coulombic component), and on quantum-derived effects on its second italicized component.

Eq. 10 $$F[\rho]=T[\rho]+V_{ee}[\rho],\ \text{where}\ V_{ee}[\rho]=J[\rho]+(V_{ee}[\rho]-J[\rho])$$

5.1.2.1.Kohn-Sham equations and exchange-correlation energy

Kohn and Sham (KS) determined the commented universal functional expression considering a fake n-electronic system, where the ground state electronic density ρ_0^{KS} is assumed to be specifically the same as ρ_0 value for the real system. For this unreal system (where no interaction between electrons is considered), the hamiltonian ($\hat{H}^{KS}$) is given as sum of the i mono-electronic KS operators ($\hat{h}^{KS}$) (see Eq. 11). Note that the first term responds to kinetic electronic energy and v^{KS} refers to the external potential assuming nuclear attraction and electronic repulsion effects over ρ.

Eq. 11 $$\hat{H}^{KS}=\sum_{i=1}^{n}\hat{h}^{KS}(\vec{r}_i)=\sum_{i=1}^{n}-\frac{1}{2}\nabla^2(\vec{r}_i)+\sum_{i=1}^{n}v^{KS}(\vec{r}_i)$$

Kohn-Sham iterative equation, analogue to the HF equation, is shown in Eq. 12. The used KS spinorbitals $\psi_i^{KS}(\vec{\omega}) = \phi_i^{KS}(\vec{r})g(\omega)$, being the eigenstates for $\hat{h}^{KS}$ are expressed by a single Slater determinant, unconsidering then electronic interactions (see Eq. 13 for ground state). The kinetic energy functional for the fictitious system $T^{KS}[\rho]$ and $J[\rho]$ can be determined by solving the KS equation, representing the well-defined part of the mentioned universal functional, whose general expression is shown in Eq. 14.

Eq. 12 $$\hat{h}^{KS}(\vec{r})\psi_i^{KS}(\vec{\omega}) = E_i^{KS}\ \psi_i^{KS}(\vec{\omega})$$

Eq. 13 $$\phi_0^{KS}(\vec{\omega}_1, \ldots, \vec{\omega}_n) = 1/\sqrt{n!}\ \left|\psi_1^{KS}(\vec{\omega}_1)\ldots\psi_n^{KS}(\vec{\omega}_n)\right|$$

Eq. 14 $$F[\rho] = T^{KS}[\rho] + J[\rho] + E_{xc}[\rho]$$

$E_{xc}[\rho]$ refers to the unspecific exchange-correlation functional, being the contribution that post-HF methods aim to introduce as a correction to HF energy calculation. A couple of terms are participating in $E_{xc}[\rho]$ such that $E_{xc}[\rho] = E_x[\rho] + E_c[\rho]$, being the exchange and correlation functionals, respectively. However, there is no explicit expression for $E_{xc}[\rho]$ and different approximations have been proposed, namely LDA (local density approximation) giving E_{xc}^{LDA}, GGA (generalized gradient approximation) giving E_{xc}^{GGA} and LSD (local spin density) giving E_x^{LSD}.

5.1.2.2. B3LYP method

If it is assumed that both contributions on total energy exchange-correlation energy can be analysed independently, it is possible to mix different expressions for the proposed functionals and the HF exact exchange functional. These are known as hybrid functionals, and by parameterisation of the coefficients different methods can be derived using the previously mentioned type of functionals.

The B3LYP method [26] expresses the exchange-correlation energy as a hybrid functional (see Eq. 15), where E_c^{VWN} functionals are used for local terms (LDA), while E_c^{LYP} functional is given by GGA approaches used for non-local correlative terms.

Eq. 15 $$E_{xc}^{B3LYP} = E_x^{LSD} + a_0(E_x^{exact} - E_x^{LSD}) + a_x \Delta E_x^{BE88} + E_c^{VWN} + a_c(E_c^{LYP} - E_c^{VWN})$$

The B3LYP functional in its unrestricted formalism will be employed in all optimisations and energy calculations.

5.2. MOLECULE-BASED MAGNETS

Better known as molecular magnets, these are an unconventional kind of magnetic materials due to their carbon-based structures, drastically differing from common metal-based magnets where the interaction takes place between two or more metallic units. However, the understanding of these inorganic magnets allows us to interpret the magnetic interactions that could appear in molecule-based magnets.

Just the same as polynuclear inorganic magnetic materials, when two or more magnetic centres interact with each other, three different cooperative effects can result. Low temperatures enable cooperations, meaning that over certain temperature range such effects cannot be seen. Ferromagnetism (represented in Fig. 3a) appears when the spins are aligned in parallel below the Curie temperature T_C. On the contrary, if the alignment between magnetic centres is antiparallel below the Neel temperature T_N , antiferromagnetism will result (see Fig. 3b). When different magnitude on spin angular momenta for magnetic centres is considered, antiparallel coupling results in a partial cancelation for those mentioned spin values, producing ferrimagnetism (represented in Fig. 3c).

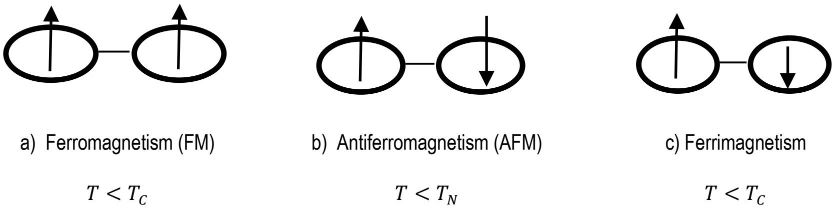
a) Ferromagnetism (FM) $T < T_C$

b) Antiferromagnetism (AFM) $T < T_N$

c) Ferrimagnetism $T < T_C$

Fig. 3: Different magnetic interactions from cooperative effects existing below certain temperature

Keeping these ideas in mind, when the units acting as magnetic centres are molecular radicals with unpaired electrons, residing in Singly Occupied Molecular Orbitals (SOMO), same interactions as Fig. 3 could be derived. Even so, it must be taken into account that in molecular magnetism, ferrimagnetism phenomena cannot be observed in pure organic magnets because the magnitude of the spin carriers for radicals is the same, s = ±1/2. Therefore, the resulting interaction will only depend on the direction of spin alignment, whether if parallel (or as parallel as possible that we can consider so) or antiparallel. Ferrimagnetism in organic compounds can be observed when a coordination complex is considered. Looking at the initial BTBN structure, two radicals (TTF and NN) can be recognised. Thus two SOMOS are present in there and, similar to Fig. 3a-b, two possible coupling modes between spin states can be predicted (Fig. 4). Given that these 2 interacting SOMOs belong to the same molecular structure, the resultant coupling mode implies a difference in the total spin multiplicity number ($\mathrm{M}=2S+1$) of the electronic state for the analysed molecule.

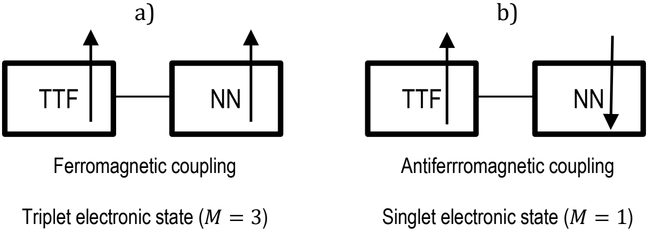

Fig. 4: Spin multiplicity states derived from different possible coupling schemes between SOMO's of the radicals, being a) triplet and b) singlet.

Thus, the desired ferromagnetism only is achieved when the electronic configuration on the ground state is given by the triplet state, whereas antiferromagnetic behaviour results from singlet ground states.

5.2.1. Spin polarization mechanism in molecule-based magnets

Assuming that the ground state multiplicity for a given diradical structure corresponds to a triplet, a FM interaction could be achieved. Each SOMO acts as a magnetic orbital if the radical has only 1 unpaired electron. Each one is mainly located over its respective radical area; these zones are then richer in spin density for the electrons existing there. This phenomenon, which molecular magnets exhibit, is known as spin-polarisation (SP). It is defined as the difference between the number of electrons existing in up (α) and down (β) spin directions (see Eq. 16).

Eq. 16 $$\mathrm{SP}= |\mathrm{n}\uparrow - \mathrm{n}\downarrow| \neq 0$$

In molecular-based magnets, the electrons angular momenta may be aligned, in part, as a consequence of the spin-polarised and induced currents established between magnetic sites. This electronic interaction also enables a D radical with higher spin-density to provide part of this density to another radical A aiming an enhanced magnetic response. Conjugated systems are responsible for this electronic conduction, given mainly through bonds by pπ-pπ interactions, but also across space when SOMOs are partially overlapped. Couplers (C) are the structures that connect both radicals and their role is to mediate for the electronic interactions to take place.

SP effect can be well described by means of DFT. The electronic density $\rho(\vec{r})$ is separated in two terms corresponding to the electronic α or β spin-specific densities, according to Eq. 17:

Eq. 17 $$\rho(\vec{r}) = \rho_\alpha(\vec{r}) + \rho_\beta(\vec{r})$$

This means that for spin-polarised systems (namely, for systems where $|\rho_\alpha(\vec{r})| \neq |\rho_\beta(\vec{r})|$) the spin density $\rho_s(\vec{r})$ can be expressed as Eq. 18 does, in which positive values indicate up spin domain and vice versa.

Eq. 18 $$\rho_s(\vec{r}) = \rho_\alpha(\vec{r}) - \rho_\beta(\vec{r})$$

In radicals, charge transfer effect produces a flux of charge and spin carriers, leading to the coexistence of conductivity and magnetism, making them perfect candidates applicable in spintronics. It uses not only the negative charged flow of electrons but also the certain spin value for this current, differing from typical electronics. Generated spin-polarised currents in materials can be affected by an external magnetic field or temperature, achieving then magnetoresistance.

5.2.2. Designing molecule-based magnets

> *Molecular design is the application of all techniques leading to the discovery of new chemical entities with specific properties required for the intended application.*
>
> *PAC, 1997, 69, 1137. (Glossary of terms used in computational drug design (IUPAC Recommendations 1997)) on page 1146*

Basic ideas of the conventional organic synthetic methodologies can be used to modify the building blocks or tune the molecule-based magnetic topology, altering electronic structures and, in turn, related properties. Indeed, to design reasonable alternatives to BTBN, other ideas apart from parallel coupling and the SP mechanism are taken into account [4]:

i. The persistence of the spin-containing radicals acting as building blocks is needed. This means that when isolated, these spin-containing radicals have to present the same electronic structure and properties than when taking part of the organic diradical entity.
ii. Mechanisms enabling an optimal coupling between the spin-containing building blocks. Intra- and inter-molecular interactions must be analysed.
iii. Propagation of the magnetism along different dimensions on the solid.

Even it being mentioned, no intermolecular interactions are studied in this work (*i.e.:* points (ii) and (iii) above are omitted). However, the information related may be considered during the design process, aiming at presenting favourable intermolecular interactions for a given hypothetical successful proposal.

With this intention, the following paragraphs are meant to describe the basics to understand the conductivity and magnetism from the spin-polarised donor radicals in the solid state. The solid-state structure for these magnets consist in the packing of mixed valance (MV) state radicals, in a way that the building diradical blocks (*e.g.* BTBN) have to coexist on the crystalline structure with different oxidation states. For the considered BTBN, the MV moiety is TTF, acting in the oxidation states shown previously in Fig. 1. The instability for these $TTF^{+\bullet}$ radicals provokes charge transfer processes between neighbour BTBN units, constantly showing redox processes (on TTF) between the π-π stacked radicals. These redox reactions take part obeying to an intermolecular migration of the aromatic system mechanism on $TTF/TTF^{+\bullet}$ [5], shown in Fig. 5. Thus, BTBN radical acts as an electron donor, transferring it to the $BTBN^{+}$ neighbour diradical.

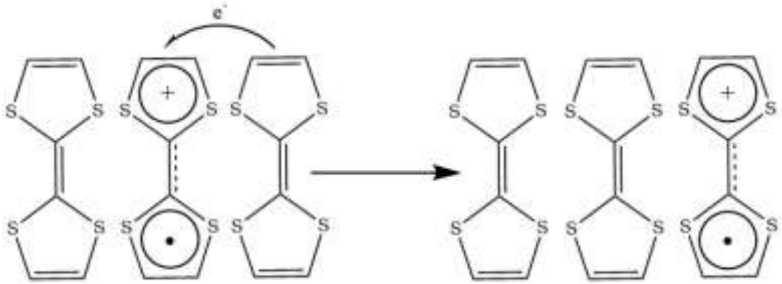

Figure 5: Intermolecular migration for the aromaticity in columnar π-stacked TTF units

5.3. APPLICABLE METHODS IN MOLECULE-BASED MAGNETS TO EVALUATE ENERGIES

5.3.1. Broken symmetry (BS)

As commented on previous sections, molecular magnets like BTBN are often large systems involving certain localised spin-polarised orbitals.

Electronic correlation effects (mutual interactions between electrons) can be distinguished, among others, between dynamic and non-dynamic [6]. Dynamic correlation is used in tight-paired electrons, whereas non-dynamical must be accounted for when there are two or more electronic configurations taking a notorious representation. The last one causes the spin localisation, so non-dynamic effects should be considered for a proper description of the electronic structure of BTBN and derived structures.

The standard methods for estimating these effects are based on considering multiple electronic configurations (*i.e.* Slater determinants) that coexist. As said, the number of equations to be solved rise exponentially and so does CPU cost.

Considering a monodeterminantal method (*e.g.* HF or DFT), the wavefunction Φ is expressed by a unique Slater determinant in terms of different spinorbitals ψ_i , see Eq. 19:

Eq. 19 $$\Phi(\vec{\omega}_1, \ldots, \vec{\omega}_n) = 1/\sqrt{n}\,|\psi_1(\vec{\omega}_1)\ldots\psi_n(\vec{\omega}_n)|$$

Different considerations can be made about the coordinates used to describe spinorbital functions in Eq. 19. When the same spatial coordinates are considered for the paired α-β electrons due to Pauli's exclusion principle, the restricted (R) scheme is applied. In this case, both α and β orbitals are degenerate so there is a certain spin symmetry. On the contrary, the fact of splitting up and down spins into different spatial coordinates is known as the unrestricted (U) description. Radical moieties treated in this work are open-shell structures (O). Comparison of RO (restricted open-shell, Fig. 6a and Eqs. 20a) and U (unrestricted open-shell, Fig. 6b and Eqs. 20b) electronic descriptions shows the inherent differences on both methods. Accordingly, we are interested in using an unrestricted treatment of the systems under study in this TFG.

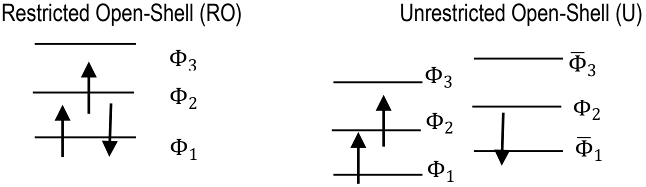

Fig. 6. (a) Restricted and (b) unrestricted description of the spinorbitals in an open-shell electronic structure consisting in 3 electrons and 3 orbitals.

$$\psi_1(\vec{\omega}_1)=\alpha\Phi_1(\vec{r}_1) \qquad \psi_1(\vec{\omega}_1)=\alpha\Phi_1(\vec{r}_1)$$

$$\psi_2(\vec{\omega}_2)=\beta\Phi_1(\vec{r}_2) \qquad \psi_2(\vec{\omega}_2)=\beta\bar{\Phi}_1(\vec{r}_2)$$

$$\psi_3(\vec{\omega}_3)=\alpha\Phi_2(\vec{r}_3) \qquad \psi_3(\vec{\omega}_3)=\alpha\Phi_2(\vec{r}_3)$$

Eqs. 20a) Eqs. 20b)

Broken symmetry (BS) methods can be used to approach, with lower computation cost, the electronic energy for spin-localised systems [7], where static correlation effects cannot be left out. To do it, BS methods take advantage from the spin symmetry loss in unrestricted methods with respect the restricted schemes. Therefore, only U descriptions are valid for BS methods. For the kind of the electronic arrangement in the analysed radical molecules, its description (especially for singlet states) is better given by the broken symmetry formalism.

Two different situations can be contemplated for the open-shell singlet (as shown in Fig. 7). The unrestricted methods cannot differ between the singlet electronic arrangements shown in black or in red, so both of them have the same energy (Fig. 7a). When the BS method is used, the symmetry loss is represented, resulting in a diradical singlet where the electronic configurations represented in black and red has no long the same energy. This allows a more faithful description for the singlet states in molecular magnets, so that the resulting singlet is the more stable of the two considered (black/red).

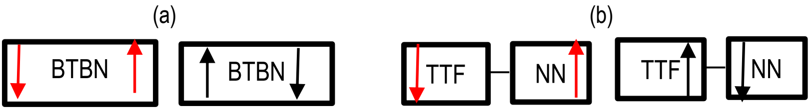

Fig. 7. (a) BTBN singlet state under a restricted description. (b) BTBN diradical singlet state under BS.

Therefore, the triplet states will be correctly described by pure unrestricted methods, whereas the BS formalism must be used for the open-shell singlet electronic states for the radical structures considered in this work. Given the fact that BS state wavefunction is not an eigenfunction of the Heisenberg Hamiltonian given the loss of degeneracy of spin symmetry related states, it can be rather better described as a half-half mixture of the BS-singlet and triplet states.

5.3.2. Heisenberg Hamiltonian

Applying Hamiltonian operators $\hat{H}$ over a set of wavefunctions describing a given quantum-mechanic state, its energy is obtained. The J_{AB} magnetic coupling between two radicals A and B can be evaluated by energy calculations using Heisenberg Hamiltonians in Eq. 21:

Eq. 21 $$\hat{H} = -2J_{AB} \cdot \hat{S}_A \cdot \hat{S}_B$$

The eigenfunctions of this Heisenberg Hamiltonian are also eigenfunctions of $\hat{S}^2$ and $\hat{S}_z$. For instance, if a diradical is considered, total spin angular moment S is directly related to the energy difference between two different spin multiplicity states, as can be seen in Eq. 22:

Eq. 22 $$E_{S=1} - E_{S=0} = -2J_{AB} = E^T - E^S$$

The value of the magnetic coupling exchange interaction J_{AB} can then be calculated if energy values are known for the triplet and singlet optimised states, using either multiconfigurational approaches that allow a better description or DFT methods, which computationally are a less demanding option.

5.3.2.1. Noodleman solutions for BS states

Noodleman once considered the case in which only two magnetic orbitals interacted [8]. Using spin-polarisation and the unrestricted formalism between up and down electrons in order to find an approximate solution, Noodleman proposed to use one single Slater determinant to calculate the singlet state energy according to the so-called BS approach.

According to Noodleman, the magnetic coupling between any two radicals, J_N (where N stands for Noodleman), can be calculated using Eqs. 23-24 [9]:

Eq. 23 $E^{S}\text{-}E^{T}=2J_N = 2(E^{S}_{BS}\text{-}E^{T})/(1+{S_{ab}}^{2})$

Eq. 24 $J_N= (E^{S}_{BS}\text{-}E^{T})/(1+{S_{ab}}^{2})$

Note that S_{ab} is the overlap between a and b SOMOs belonging to radicals A and B (see Eq. 25 for equivalent definition). This integral is in some way, a magnitude to evaluate the ability for those SOMOs to practice the electronic transfer through space. As seen, FM interaction given by triplet ground states is favoured when those SOMOs present no overlap between them. Two limiting situations can be derived from Eq. 24 (see Eq. 26 and Eq. 27).

Eq. 25 $S_{ab}=\langle\psi_a^{SOMO}|\psi_b^{SOMO}\rangle$

Eq. 26 Non-overlapped SOMOs: $S_{ab}\approx 0\rightarrow J_N= (E^{S}_{BS}\text{-}E^{T})$

Eq. 27 Overlapped SOMOs: $S_{ab}\approx 1\rightarrow J_N= (E^{S}_{BS}\text{-}E^{T})/2$

5.3.2.2. Yamaguchi solutions for BS states

Yamaguchi developed a BS mathematic solution concluding with an expression capable for the J_{AB} value calculation, expressed as J_Y and corrected including approximate spin-projection methods. His method is also valid for the study of multiple magnetic centres interacting, so it can be used in more general cases than Noodleman's approach.

According to Yamaguchi's method, initial Heisenberg Hamiltonian shown in Eq. 21 is expressed in terms of total spin operator, $\hat{S}= \hat{S}_A+ \hat{S}_B$, becoming Eq. 28 [7]:

Eq. 28 $\hat{H}= -2J_{AB}\,(-\hat{S}^2+ {\hat{S}_A}^{2}+ {\hat{S}_B}^{2})$

Operating the Heisenberg Hamiltonian in Eq. 28 on a wavefunction describing the BS state in singlet (S) and triplet (T) multiplicities, the energies of these states can be expressed as seen in Eq. 29 and Eq. 30, respectively.

Eq. 29 $$\langle \varphi_{BS}^{S} | \hat{H} \varphi_{BS}^{S} \rangle = E^{S} = J_{AB} \left(-\langle \hat{S}^2 \rangle^{S} + \langle \hat{S}_A{}^2 \rangle^{S} + \langle \hat{S}_B{}^2 \rangle^{S} \right)$$

Eq. 30 $$\langle \varphi_{BS}^{T} | \hat{H} \varphi_{BS}^{T} \rangle = E^{T} = J_{AB} \left(-\langle \hat{S}^2 \rangle^{T} + \langle \hat{S}_A{}^2 \rangle^{T} + \langle \hat{S}_B{}^2 \rangle^{T} \right)$$

As mentioned previously, spin contamination on the triplet states can be neglected due to the almost equal values between triplet states $\langle \hat{S}^2 \rangle_{exact}{}^{T} \cong \langle \hat{S}^2 \rangle_{BS}{}^{T} \equiv \langle \hat{S}^2 \rangle^{T} \cong 2$. Singlet states present opposite behaviour throughout these considerations. It thus follows that the spin-contamination effect must be considered only for singlet states (or in general for low-spin states). When being under these circumstances and according to the spin projected procedure in Yamaguchi's method, the energy gap between different spin multiplicity states can be expressed as shown in Eq. 31, where J_{AB} has been corrected in terms of spin-contamination errors. Yamaguchi's method considers the high-spin (HS) and low-spin (LS) states:

Eq. 31 $$E_{BS}^{LS} - E^{HS} = 2J_{AB} - J_{AB} \langle \hat{S}^2 \rangle_{BS}^{LS} \text{ where } 2 = \langle \hat{S}^2 \rangle^{HS} \text{ since } HS = T$$

The extension of Eq. 31 to a system where two spin units coexist and interact resulting in different spin multiplicity states, one higher (HS) than the other (LS), leads to the Yamaguchi expression for J_{AB} magnetic couplings, J_Y (see Eq. 32, where Y stands for Yamaguchi).

Eq. 32 $$J_Y = (E_{BS}^{LS} - E^{HS}) / (\langle \hat{S}^2 \rangle^{HS} - \langle \hat{S}^2 \rangle_{BS}^{LS})$$

Note that Eq. 32 is derived under DFT formalism, and is applicable to systems with multiple spins centres.

5.3.3. McConnell I mechanism

Far from the mathematical application of Heisenberg Hamiltonians, McConnell I mechanism is widely-accepted to qualitatively predict the magnetic interactions between spin carriers in solid-state structures.

The unpaired electron density on radicals is distributed all over their chemical structure, bearing the consisting atoms with a certain spin density (ρ_s). The radical is then spin-polarised, and positive and negative values are possible for those ρ_s depending on the α, β atomic spin-domain, respectively. The McConnell-I mechanism states that, given two neighbouring unpaired electrons corresponding each one to a different open-shell molecule, the exchange interaction is:

- Ferromagnetic ($J>0$) when the major overlap between the spin density from one and other radicals takes place between opposite sign spin densities, $\rho_{\pm} \leftrightarrow \rho_{\mp}$
- Antiferromagnetic ($J<0$) when the spin densities involved on the interaction have the same sign, $\rho_{-} \leftrightarrow \rho_{-}$ or $\rho_{+} \leftrightarrow \rho_{+}$

This mechanism will be qualitatively used for both proposing building blocks and assessing magnetic behaviour between the new *in silico* radicals proposed in this TFG.

6. COMPUTATIONAL PROCEDURE

All of the structures and molecules analysed during this work have been studied following the same general steps exposed in this section.

Initially the structure is drawn with Avogadro [10a,10b]. A first geometry optimisation is carried out with the Auto Optimize tool from Avogadro using the Universal Force Field (UFF) with the steepest descendent algorithm, in order to get a good guess of the geometry by considering the connectivity and hybridisation of each atom on the periodic table [11].

The coordinates of this pre-optimised structure are used as input for stricter geometry optimisation calculations using Gaussian [12], where important variables like spin multiplicity are now considered, differing from UFF in Avogadro. Geometry optimisations will be made in order to find the parameters (bond distances, angles and dihedral angles) with the minimum associated electronic energy, representing a minimum on the PES of the molecule under study. Frequency calculations will be also carried out to verify that the optimised structure is a minimum, *i.e.* that no imaginary frequencies are found.

All Gaussian calculations are done at UB3LYP/6-311+G(d,p) level. This means that the DFT-B3LYP monodeterminantal method was chosen, using the expression for the correlation-exchange functional for the electronic density shown in Eq. 15. The U in UB3LYP stands for the unrestricted description of spinorbitals required for a proper description of molecular magnets, and the broken symmetry BS approach is used to describe the analysed open-shell systems. The 6-311G+(d,p) term provides the description of the atomic orbitals basis set functions used to build, by linear combination (LCAO), the KS spinorbitals used in the UB3LYP calculation. This term indicates the use of 3 basis functions for each atomic orbital using 5 primitive Gaussian-type orbitals (GTO) with 3+1+1 contraction on the valence orbitals. Polarisation functions have been also considered in order to describe the loss of spherical geometry for the electronic space because of the presence of the others atoms on the molecule. Orbitals d for non-H atoms and p for Hydrogen atoms are the polarisation functions added, shown in parenthesis in the respective term (d,p). Diffusion functions have also been considered for non-H atoms aiming at giving a better description of the areas far away from the nuclei, indicated using the + sign.

Once the geometry is confirmed to be a minimum on the PES, the J_{AB} magnetic coupling data will be extracted from calculations. Energy values for the different spin multiplicities will be used to determine whether the behaviour for the given structure is FM or AFM. To do so, Noodleman solutions for the BS states (see Section 3.3.2.1) are considered in order to provide a first approach to this J_{AB} interaction. Data related to MOs or spin densities will be visualised using Chemcraft [13] tools. These representations for SOMOs, for instance, will enable us to do the following qualitative approach:

- When there is overlap between the SOMOs involved, total overlap is considered ($S_{\mathrm{ab}}=1$), no matter what the real S_{ab} magnitude is. Then, J_{AB} expression corresponds to the Eq. 27
- When there is no overlap, ($S_{\mathrm{ab}}=0$), J_{AB} is expressed as in Eq. 26

The *in silico* BTBN-based proposals showing a very large improvement on FM with respect to BTBN will be further assessed in order to estimate a more precise value for the J_{AB} magnetic couping. Therefore, using the same calculated energy values, Yamaguchi's framework will be applied to the calculation of the corresponding magnetic coupling to compare with Noodleman's.

7. RESULTS AND DISCUSSIONS

Before designing any BTBN-based structure, BTBN itself and its building blocks (namely, TTF and NN) should be studied in order to fully understand its ferromagnetic behaviour. From this analysis on, different molecules will be proposed with the objective of enhancing the FM coupling shown by BTBN. Evaluation of the J_{AB} magnetic coupling in terms of singlet and triplet energies will finally reveal the magnetic behaviour for each proposal. Hereafter, Singly Occupied Molecular Orbitals (SOMO) as well as spin density data will be used to analyse and interpret the results of our calculations.

In order to designate a systematic name to the structures proposed, note that the design is done targeting either acceptor, coupler or donor building blocks (A, C or D) aiming at seeing its particular effect. The different structural units are then designed as Ai, Cj or Dk where i, j and k are the index numbers referring to a given specific building block for a so-called AiCjDk proposal. The set for A-type radicals can be seen in Fig. 8, C-type in Fig. 9, and D-type in Fig. 10. Wavy bonds drawn in many of the structures indicate the bonding position with a given adjacent building block. Radicals TTF and NN in BTBN will be individually studied and this is why they have a specific name: $TTF^{+\bullet}$ in A0 is different from the di-bromo $TTF^{+\bullet}\sim$ unit shown in A1 (both in Fig. 8), HNN radical in D0 is slightly different from ∼NN building block in D1. After that, structures emerging as combinations between the most promising A, C and D units will be also considered. Accordingly, BTBN is designed with the name A1C1D1, and all the proposals will be called with the P letter as a prefix for "Proposal" followed by the different AiCjDk units shown above.

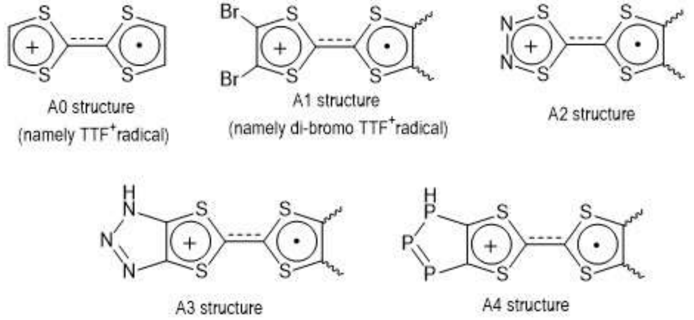
A0 structure (namely TTF^{+}radical)
A1 structure (namely di-bromo TTF^{+}radical)
A2 structure
A3 structure
A4 structure

Fig. 8: Set of A-type moieties considered (i= 0, 1… 4)

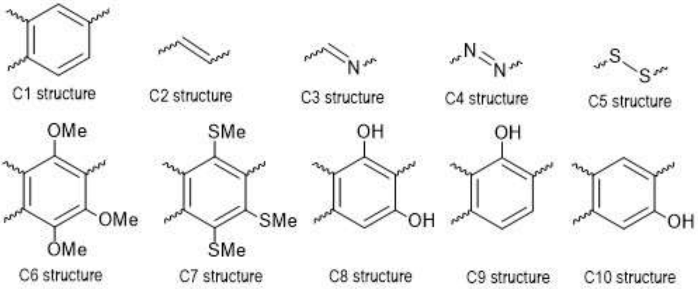

C1 structure C2 structure C3 structure C4 structure C5 structure

C6 structure C7 structure C8 structure C9 structure C10 structure

Fig. 9: Set of C coupler structures considered (j=1, 2 … 10)

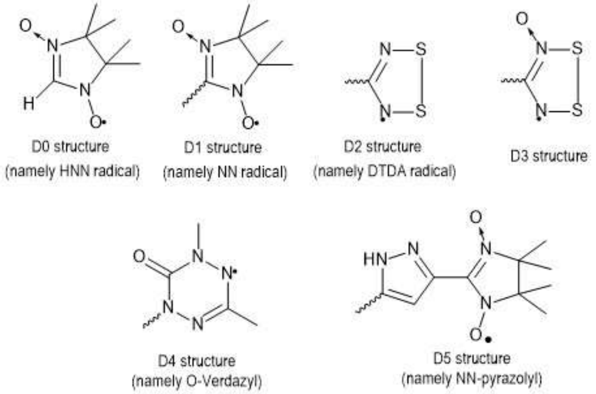

D0 structure (namely HNN radical) D1 structure (namely NN radical) D2 structure (namely DTDA radical) D3 structure

D4 structure (namely O-Verdazyl) D5 structure (namely NN-pyrazolyl)

Fig. 10: Set of D-type radicals considered (k=0, 1 … 5)

7.1. BTBN (A1C1D1)

BTBN is set up from the TTF$^{+\bullet}$ and NN radicals, that will be independently (*i.e.* A0 and D0) as well as cooperatively (*i.e.* A1C1D1 in Fig. 2) studied. The idea is to identify the effects favouring the FM behaviour in BTBN and, by comparison, justify the magnetic behaviour predicted for the proposals.

The A0 (TTF$^{+\bullet}$) α-SOMO single electron responsible for the doublet multiplicity is located all over the molecule and presents a nodal molecular plane that inverts the sign of the π orbital lobes (see Fig. 11a). At the same time, positive lobes on all S atoms are not interacting with the negative lobes in C=C bonds on the same molecular plane. The spin density is distributed all along the molecule showing the same nodal plane, but without sign inversion (see Fig. 11b). All 4 S atoms have the same maximum spin density value. Notable spin density is also detected on the C=C mid-bond. HOMO coefficients for the carbons on the external double bond have approximately the the same value (differing in the 4th decimal place). Therefore all four carbons are good sites for bonding other structures with potential ability to modify the electronic structure and polarise the spin on $TTF^{+\bullet}$. This evidences the chemical equivalence due to symmetry. Obviously if a functional group is bonded to those sites, the simmetry decreases and the last statement will not be true.

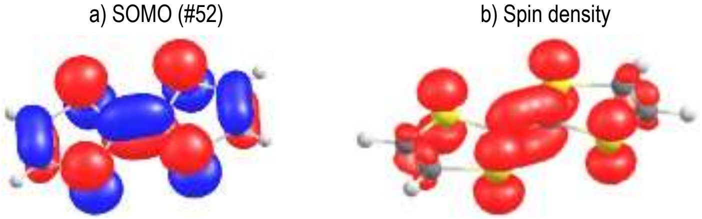
a) SOMO (#52)

b) Spin density

Fig. 11. $TTF^{+\bullet}$ (A0): (a) Singly Occupied Molecular Orbital, and (b) spin density.

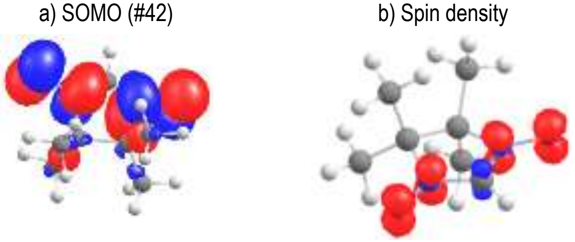
a) SOMO (#42)

b) Spin density

Fig. 12. HNN (D0): (a) Singly Occupied Molecular Orbital, and (b) spin density

The spin density on the NN radical results from an unpaired electron on the electronic structure, mainly located over the O atoms of this D0. Thus, it is found on a doublet ground state. The representation of the α-SOMO responsible of this lone electron shows that it can be mainly located over the N, O atoms (see Fig. 12a). Like in A0, a nodal plane appears with sign inversion on each side and different sign also for adjacent N-O lobes. The spin density is located on $O^{\delta+}$-$N^{\delta+}$-$C^{\delta-}$-$N^{\delta+}$-$O^{\delta+}$, where the unrepresented C in SOMO connecting NO bounds adopts negative spin density (see Fig. 12b). However, the coefficient for the specified C atom is large enough to be considered as a good bonding site, capable for the electronic interactions between parts linked.

The union of these two radicals using a benzene (C1) as a spacer and electronic coupler results in BTBN diradical (A1C1D1), for whom two multiplicity states have to be considered (namely, S (singlet) and T (triplet)). The addition of two bromine atoms linked to the dithiole ring (A1) was designed by *Komatsu et al* [15] in order to increase the intermolecular interactions in the crystal. The S- and T- SOMOs are shown in Fig13a-b respectively : note that for the triplet state the overlap between SOMOs could be practically neglected ($S_{\mathrm{ab}}=0$), while for the S- state it could not ($S_{\mathrm{ab}}\neq 0$) .For the sake of calculating values of J_{AB} magnetic coupling, we will assume that $S_{\mathrm{ab}}=1$, which will produce a lower bound for J_{AB}. The spin-density, wich can also be quantitatively evaluated to provide information about SP, is also visualized in Fig. 13c-d for S and T states. Note that ρ_s inverts on NN for the different states. It can be also seen that those ρ_s in A1C1D1 are in agreement with the ones seen in the isolated radicals. According to this observation, A0 and D0 are persistent radicals, satisfying the only intramolecular requirement considered (see (i) in Section 5.2.2) for radicals used as building blocks in molecular magnets design

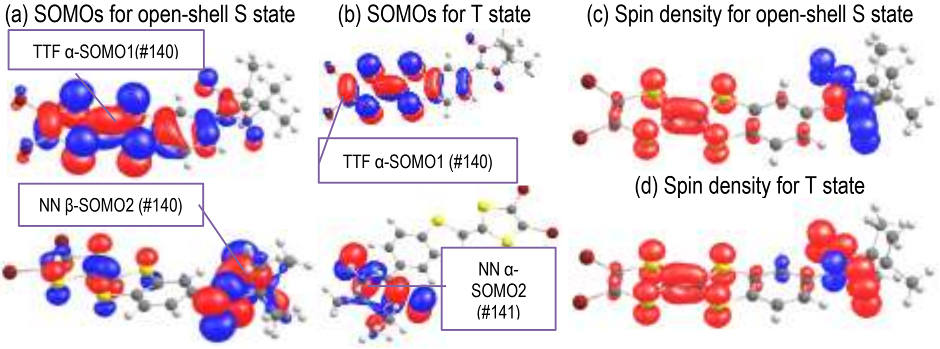
(a) SOMOs for open-shell S state
(b) SOMOs for T state
(c) Spin density for open-shell S state
(d) Spin density for T state

Fig. 13: (a-b) SOMOs and (c-d) spin-density distribution for open-shell singlet S and triplet T states, respectively, of A1C1D1 (BTBN).

The estimated magnetic coupling using Eq27 (Noodleman, considering $S_{\mathrm{ab}} = 1$ overlapped SOMOs) for BTBN is $J_{N,\, BTBN} = 56.36\ \mathrm{cm}^{-1}$

The spin density distribution reveals the SP mechanism topologic differences along the structures for each state. Enhanced FM results when there is a strong spin-electronic interaction between radicals at the triplet state. Spin polarisation SP is the mechanism that allows this interaction between different magnetic units, and it is favoured when the spin density sign between adjacent atoms is inverted. The moieties present an opposite sign between them on the bonding atom, and the coupler C1 presents a through-bond “path” connecting both units *via* the SP mechanism. Hence, the spin multiplicity state exhibiting a more enhanced SP mechanism along the coupler, *i.e.* connecting magnetic spins between units in the diradical, will indicate the magnetic ground state of each proposal: as mentioned, FM will be achieved for triplet states, whereas AFM will result for the singlet states.

In the following sections, the designed proposals and their *in silico* predicted magnetic coupling will be discussed and compared to A1C1D1 (BTBN) in order to find both a reasonable and best suited structure for applications in the spintronics field.

7.2. MODIFYING A-TYPE UNIT (AIC1D1)

In this section the effect of different Ai units, keeping the C1D1 structure fixed, is carried out. The idea of any A-type radical is that, when being in the solid phase in a compound exhibiting magnetoresistance, it has to act as mixed valence MV enabling the transmission of unpaired electrons from one unit to another in the solid [14] . Intermolecular migration of aromaticity between different A-units on the diradical molecular magnets explains this phenomenon.

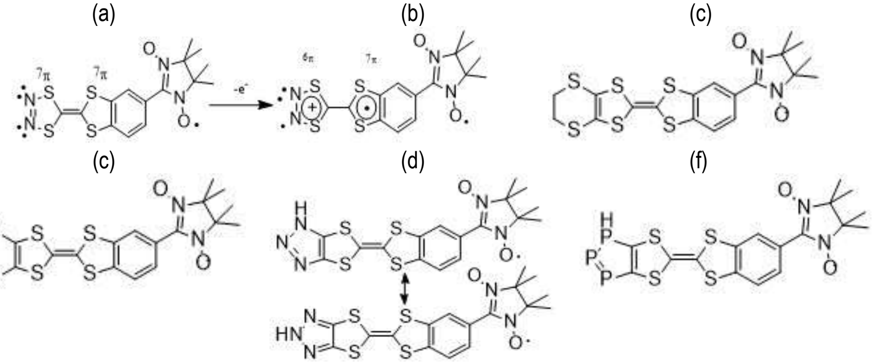

Fig. 14: Mono-oxidation of (a) pre-PA2C1D1 leading to (b) PA2C1D1. (c) ETBN molecule. (d) PA3C1D1 and its 2H-1,2,3-triazole tautomer. (e) PA4C1DD1 structure

TTF is a molecule with this mixed valence ability, resulting from the 7π-7π to 7π-6π change in the electronic structure when TTF is oxidized with one electron [5], as shown in Fig. 1. The idea for the first proposal PA2C1D1 is to replace the two hydrogenated C atoms on TTF by N, simulating the same 7π-7π to 7π-6π change as in TTF but with the N lone pairs pushing indeed the electronic density towards the C1 region (see Fig. 14a-b, where pre-PA2C1D1 is the non-oxidized PA2C1D1 diradical).

Moreover, the addition on the same carbons of the donor $-S-(CH_2)_2-S-$ group makes the electronic structure compact enough to be the first TTF-based ion-radical experimentally synthetized, named ETBN [15,16] (see Fig. 14c). Inspired by ETBN, the designed PA3C1D1 uses N atoms too in order to cause the same π-retrodonor effect because of the lone pairs. It is designed in such a way that all 3 atoms added to form the 5-membered ring are N and the TTF π-conjugated system delocalises too over these nitrogen atoms. This 1H-1,2,3-triazole group is chosen instead of the addition of 4 N atoms to form a 6-membered ring because the original planar structure in A1 would be excessively modified. In addition, aromaticity and tautomerism in this triazole ring could balance the lost stability that arises after modifying a 6 atoms ring in ETBN to 5 in this proposal. PA3C1D1 and its tautomer are shown in Fig. 14d. The PA4C1D1 (see Fig. 14e) is also inspired in ETBN: P is used now instead of N in the PA3C1D1 to aim at a better interaction with the nearest spin-polarised S atoms given that they both have principal quantum number n=3.

Comparison between $J_{PAiC1D1}$ results obtained for each in silico A1 modified PAiC1D1 proposal using Noodleman's Eq. 27 and $J_{N,BTBN}$ value is shown on Fig. 15. As seen, PA4C1D1 achieves an enhanced FM coupling between moieties($J_{N,\,BTBN} < J_{N,\,PA4C1D1}$). The spin densities distribution in this diradical reveals that, on the triplet state (see Fig. 16b), the SP mechanism observed in BTBN (Fig. 13d) and in accordance to McConnell-I also holds for this structure. It thus follows that since the triplet multiplicity turns out to be the ground state electronic structure, stronger FM is predicted for PA4C1D1 than for BTBN.

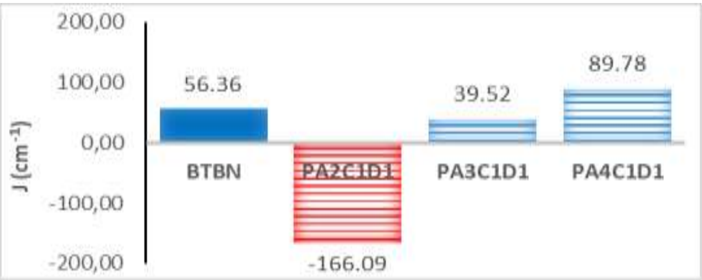

Fig15: J_N comparison between initial PA1C1D1 and PAiC1D1 structures designed in this section

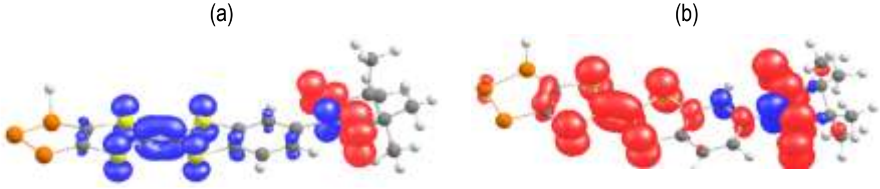

Fig. 16: Spin densities for PA4C1D1 in (a) open-shell singlet (S) state and (b) triplet (T) state

7.3. MODIFYING C-TYPE UNIT (A1CJD1)

Akin to the proposals in the section before, modifications on the inicial benzene C1 coupler are studied now with no modifications of the radicals A1 and D1.

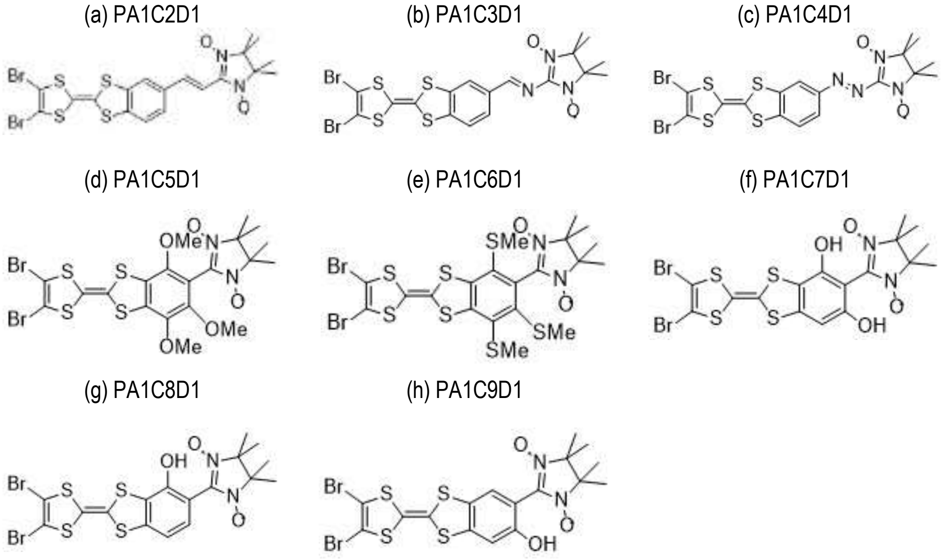

(a) PA1C2D1 (b) PA1C3D1 (c) PA1C4D1

(d) PA1C5D1 (e) PA1C6D1 (f) PA1C7D1

(g) PA1C8D1 (h) PA1C9D1

Fig. 17. Chemical structures for PA1C2D1 to PA1C9D1 proposals

For the first type of structures designed, simpler structures are used as Cj considering in its design only the most spin-polarised C atoms on C1, and preserving the bonding atoms structure as in BTBN. The simplest diradical design then, called PA1C2D1 (Fig. 17a) considers a (Z)-ethylene coupler (C=C). Structure PA1C3D1 (see Fig. 17b) considers a C=N coupler as an intermediate between C2 and the azo linker C4, leading to PA1C4D1 (Fig. 17c). This last C4 is inspired by the azobenzene couplers used in the work by *I. Ratera and J. Veciana* as photoswitchable molecular systems [4].

For the other type of proposals designed in this section, the C1 structure is not removed. Furthermore, *in silico* designed C5-C9 structures are based on the idea that increasing the electronic density on closed-shell benzene will also increase the electronic interaction between units, since it will assist the magnetic interaction. The groups considered are donors of electron density *via* resonance, although a light π retro-acceptation also exists. PA1C5D1 and PA1C6D1 consist on replacing the 3 H atoms belonging to benzene with 3 OMe or 3 SMe groups (see Fig. 17d and Fig. 17e, respectively). Hydrogen bonds have shown the ability to act as magnetic couplers between magnetic orbitals as well, mainly when metal atoms are involved in coordination compounds [4]. Mixing this idea with the one considered for the proposals before, a group of some hydroxylated phenyl α-NN that had been studied [17] is here explored. In this case, the –OH groups are bonded in ortho- (o-) position with respect NN since it is supposed to present a FM interaction, according to McConnell I model. The considered structures PA1C7D1-PA1C9D1 are shown in Fig. 17f-h respectively.

Fig. 18: J_N comparison between reference BTBN and PA1CjD1 structures designed in this section

Comparison between $J_{N,PA1CjD1}$ values obtained for each *in silico* C1 modified PA1CjD1 proposal using Noodleman's Eq. 27 and $J_{N,BTBN}$ is shown in Fig. 18. As observed, the proposals made using C2-C4 and C9 present a notable enhanced ferromagnetic coupling. Again, the SP mechanism seen for those structures in the triplet ground state recalls the same effect than for BTBN. The spin density distribution for these PA1C2D1-PA1C4D1 and PA1C9D1 are shown in Fig. 19a,b to Fig. 22a,b respectively.

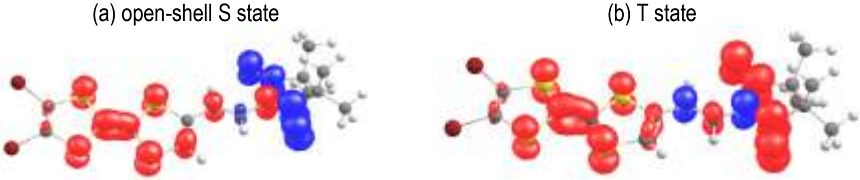
(a) open-shell S state

(b) T state

Fig. 19: Spin densities for PA1C2D1 in (a) open-shell singlet (S) state, and (b) triplet (T) state.

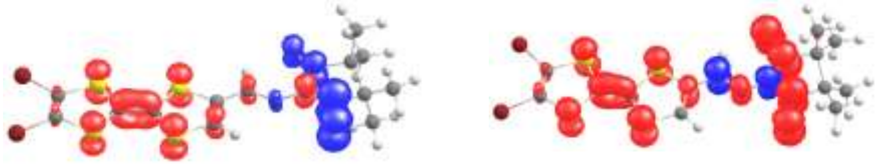
(a) open-shell S state

(b) T state

Fig. 20: Spin densities for PA1C3D1 in (a) open-shell singlet (S) state, and (b) triplet (T) state.


(a) open-shell S state

(b) T state

Fig. 21: Spin densities for PA1C4D1 in (a) open-shell singlet (S) state, and (b) triplet (T) state.

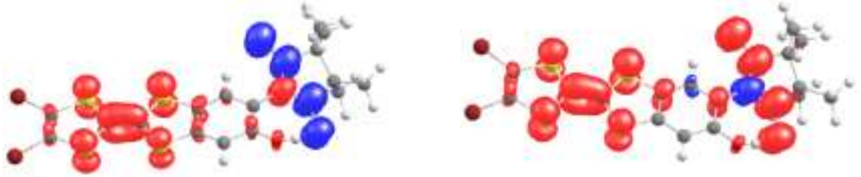
(a) open-shell S state

(b) T state

Fig. 22: Spin densities for PA1C9D1 in (a) open-shell singlet (S) state, and (b) triplet (T) state.

7.4. MODIFYING D-TYPE UNIT (A1C1DK)

In this section, D1 in A1C1D1 diradical is replaced by different Dk radicals, leading to *in silico* PA1C1Dk designed proposals.

The first PA1C1D2 shown in Fig. 23a considers the 1,2,3,5-dithiadiazolyl (DTDA) radical to replace NN. Different theoretical [18] and experimental studies [19] have confirmed the nature of localised spin density on the DTDA ring, providing the radical with conducting and magnetic properties. It is also known the tendency of these compounds to dimerisation in solid state and the influence of the bonded groups in such process [20]. Inspired in the imino-nitroxide radical [21], D3 is designed bonding an extra O to one N atom on DTDA ring in PA1C1D2, aiming at more atomic variability and leading then to PA1C1D3 (see Fig. 23b). *Oakley and coworkers* carried out studies on solid structure using a diselenazolyl DTDA analogue radical [22a] (D4), based on *Haddon's* idea that a half-filled conduction band with metallic behaviour could be achieved when the space between π-radicals in the solid state is short enough [22b]. The PA1C1D4 is designed using this di-selenium DTDA analogue radical (see Fig. 23c).

Another broadly studied purely organic radical showing SP, experimentally synthetized [4, 23] and capable to exhibit other interesting related phenomena, such as photo-excited spin alignment processes [21], is the O-Verdazyl (see D5). Given that modetare high J_{AB} couplings are predicted for TTF and D5 [9, 24], PA1C1D5 is designed (see Fig. 23d).

It is known that substituted pyrazolyl nitronyl nitroxide (NN-Pz, D6), is mainly AFM when coordinated to certain metal atoms [25]. This radical ligands can even be used to form chelate structures and are thus here considered given the available methods for their selective synthesis. That would facilitate experimentation in case that magnetic behaviour becomes FM when D6 takes part in a purely organic structure (without metallic atoms); PA1C1D6 is shown on Fig. 23e.

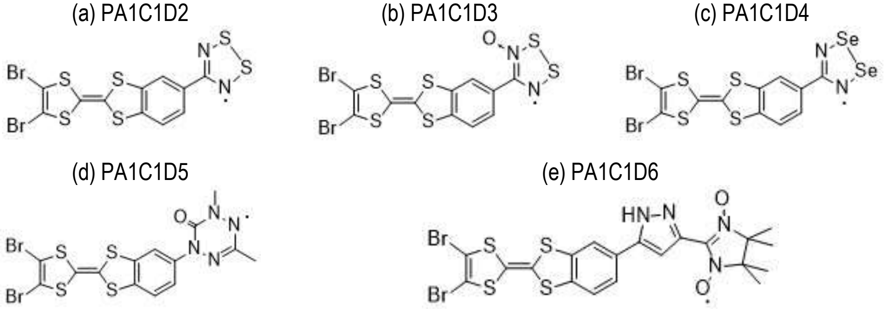
(a) PA1C1D2
(b) PA1C1D3
(c) PA1C1D4
(d) PA1C1D5
(e) PA1C1D6

Fig. 23. Chemical structures for PA1C1D2 to PA1C9D6 proposals

Fig24 :J_N comparison between initial PA1C1D1 and PA1C1Dk structures designed in this section

Comparison between $J_{N,PA1C1Dk}$ values obtained for each *in silico* D1 modified PA1C1Dk proposal using Noodleman's Eq. 27 and $J_{N,BTBN}$ is shown in Fig. 24. All PA1C1Dk proposals show an AFM behaviour. Very strong AFM is seen using the D6 NN-Pz radical, showing no modifications on magnetic behaviour also when being in a pure organic diradical. In this case, the AFM behaviour is explained by the stabilisation of the open-shell singlet state by means of the SP mechanism (except for PA1C1D3 whose AFM is extremely weak). This line of reasoning is exemplified for PA1C1D2, PA1C1D4-PA1C1D6 using the spin densities of PA1C1D5 (D5= O-Verdazyl), where this SP is clearly shown by the singlet state (see Fig. 25a-b). As said, the AFM interaction exhibited by PA1C1D3 is very small, and the spin density distribution is inconclusive to rationalise that behaviour (see Fig. 26a-b).

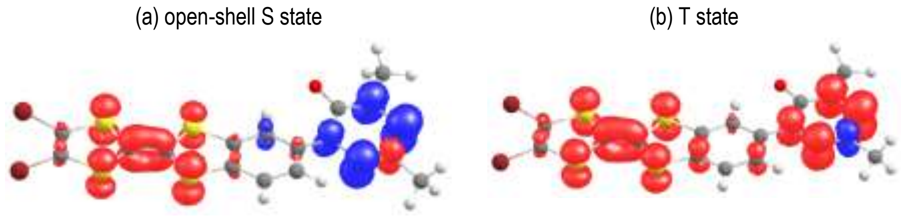
(a) open-shell S state (b) T state

Fig. 25: Spin densities for PA1C1D5 in (a) open-shell singlet S state, and (b) triplet T state.

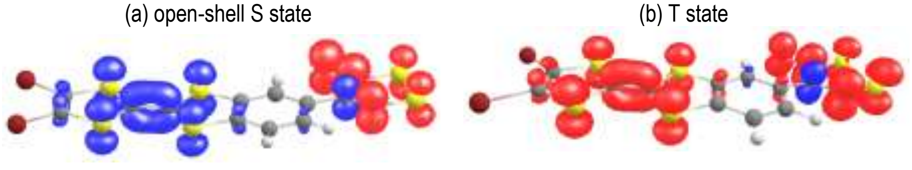
(a) open-shell S state (b) T state

Fig. 26: Spin densities for PA1C1D3 in (a) open-shell singlet S state, and (b) triplet T state.

7.5. IMPROVING FERROMAGNETISM IN BTBN-ENHANCED PROPOSALS (PEN)

This section will benefit from all previous proposals that have predicted a notorious enhanced ferromagnetic behaviour with respect to our reference, *i.e.* to BTBN. Specifically, we will focus on PA1C2D1 and PA1C9D1. Accordingly, the PEn (n=1,2 ...) proposals consist in the design of diradical structures using A1 and D1 coupled by the ethylene coupler –OH substituted. Thus, 2 different enolic couplers PE1 and PE2 are considered (one for each position of the hydroxyl group in the C=C bond, see Fig. 27a-b). The last PE3 uses an ethylene coupler with a new modified hydroxylated TTF radical (see Fig. 27c). Despite the azo C4 shows also a high FM intramolecular coupling, it is dismissed because –OH groups cannot be bonded to the N atoms.

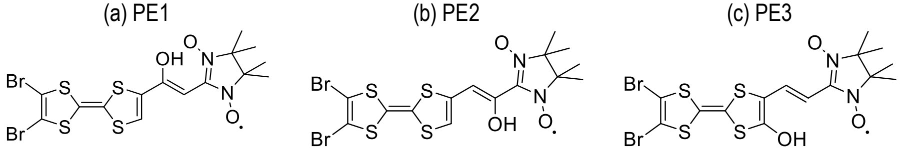
(a) PE1 (b) PE2 (c) PE3

Fig. 27. Chemical structures for PE1 to PE3 proposals

Comparison between J_{PEn} values obtained for each *in silico* PEn proposal using Noodleman's Eq. 27 and $J_{N,BTBN}$ is shown in Fig. 28a, whereas same comparison using Yamaguchi approach according to Eq. 32 is shown on Fig. 28b. Once more, the SP mechanism explains all the results obtained (see Fig. 29a,b to Fig. 31a,b for spin density distribution of PE1-PE3, respectively). Note that the spin inversion for PE3 is given in the hydroxylated TTF (A) unit designed by combination in this section, ensuring the commented capacity for the carbons on the external double bond in TTF to modify the electronic structure and polarise the spin on it. Note that the improvement in the FM behaviour shown by PE1 and PE3 proposals is very promising for future both theoretical and computational studies.

Fig. 28: Comparison between reference A1C1D1 and designed PA1C2D1, PA1C9D1 and PEn structures using either (a) Noodleman's (J_N), or (b) Yamaguchi's (J_Y) approach to calculate J_{AB} magnetic interactions.


(a) open-shell S state (b) T state

Fig. 29: Spin densities for PE1 in (a) open-shell singlet S state, and triplet T state

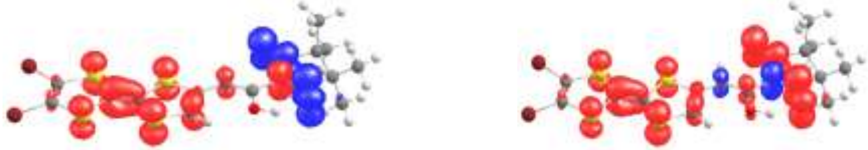
(a) open-shell S state (b) T state

Fig. 30: Spin densities for PE2 in (a) open-shell singlet S state, and triplet T state

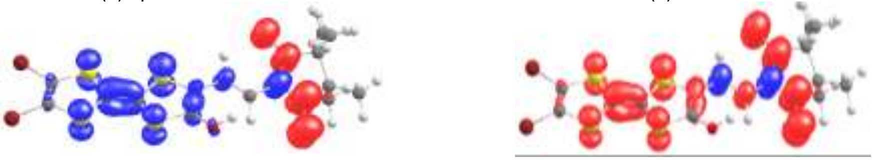
(a) open-shell S state (b) T state

Fig. 31: Spin densities for PE3 in (a) open-shell singlet S state, and triplet T state

7.6. TRIRADICAL BASED DESIGNED PROPOSALS (PTN)

On a study made by *Sugawara et al.* a ground-state quartet triradical showing spin polarisation cation was prepared [5]. It was designed using tianthrene as cation radical core extending its aromaticity through C1 rings, which mediate the intramolecular coupling between units. The so called high state multiplicity cation, 2,8-TANN2$^{+\bullet}$, is shown in Fig. 32a. The proposals PTn are inspired by this 2,8-TANN2$^{+\bullet}$ triradical, using TTF$^{+\bullet}$ instead as the A-type radical core. Hence, PT1 and PT2 (see Fig. 32b,c respectively) result from two possible position structural isomers, and are designed aiming at presenting a similar behaviour as 2,8-TANN2$^{+\bullet}$ does. Note that the idea of three radicals interacting implies that only one coupling combination of spins achieves a quartet high spin multiplicity state showing FM. By contrast, 3 different AFM interactions are available for doublet low spin multiplicity electronic states (see Scheme 2 for all 3 different Slater determinants).

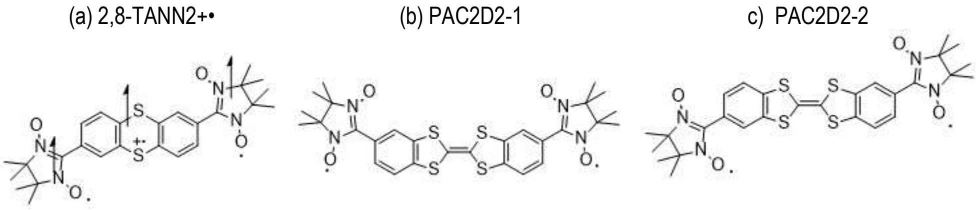
(a) 2,8-TANN2+•
(b) PAC2D2-1
c) PAC2D2-2

Fig. 32: (a) 2,8-TANN2+• triradical (M=4 quartet ground state). Proposed (b) PAC2D2-1 and (c) PAC2D2-2 triradical structures.

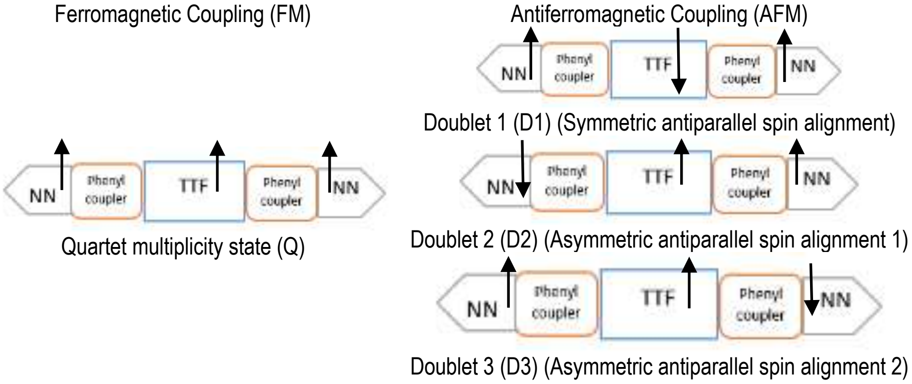
Ferromagnetic Coupling (FM)
Antiferromagnetic Coupling (AFM)
Doublet 1 (D1) (Symmetric antiparallel spin alignment)
Quartet multiplicity state (Q)
Doublet 2 (D2) (Asymmetric antiparallel spin alignment 1)
Doublet 3 (D3) (Asymmetric antiparallel spin alignment 2)

Scheme 2: Different spin multiplicity states resulting from their corresponding electronic configuration considered for PT1 and PT2 proposals.

Consequently, in these two triradical structures there are more intramolecular magnetic interactions than in the previously studied diradical proposals. Considering that the magnetic interaction is mainly through-bond, and that there is a high level of symmetry in both PT1 and PT2 proposals, the interaction between each NN radical and the centred cationic TTF radical can be considered to be the same (i.e. $E_{BS}^{D2}=E_{BS}^{D3}=E_{BS}^{D^{asym}}$, and accordingly $J_{NN\text{-}TTF} = J_{TTF\text{-}NN}$). This approximation means that the asymmetric doublets are taken to be degenerate in energy and allows considering only one of the asymmetric doublet states, simplifying the system of equations and reducing the computation cost. New equations (Eq. 33 - Eq. 35) based on Yamaguchi's spin-projected corrected solution have been developed in order to properly extract the magnetic couplings between radical units in the same molecule.

Eq. 33 $$\mathrm{E_{BS}^{D^{sym}}\text{-}E^{Q}= 2J_{Y_{(TTF/NN)}}\left(\langle \hat{S}^2\rangle^{Q}\text{-}\langle \hat{S}^2\rangle_{BS}^{D^{sym}}\right)}$$

Eq. 34 $$\mathrm{E_{BS}^{D^{asym}}\text{-}E^{Q}=\left(\langle \hat{S}^2\rangle^{Q}\text{-}\langle \hat{S}^2\rangle_{BS}^{D^{asym}}\right)\left(J_{Y,(TTF/NN)}+J_{Y,(NN_2)}\right)}$$

Eq. 35 $$\mathrm{J_{Y_{(TTF/NN)}}= (E_{BS}^{D^{sym}}\text{-}E^{Q})/2\left(\langle \hat{S}^2\rangle^{Q}\text{-}\langle \hat{S}^2\rangle_{BS}^{D^{sym}}\right)}$$

Comparison between J_{PTn} values obtained for each in silico PTn proposal and $J_{Y,BTBN}$ value is shown in Fig. 33, as well as the SP mechanism illustrated in the quartet high spin multiplicity state for both proposals (see Fig. 34 and Fig. 35). At the light of the values of $J_{Y,TTF\text{-}NN}$, it is clear that these two triradicals (PT1 and PT2) also are promising candidates for spintronics applications.

Fig. 33: $J_{Y,TTF\text{-}NN}$ comparison between reference BTBN and PTn structures designed in this section

Fig. 34: Spin density for PT1 in the resulting quartet high spin state

Fig. 35: Spin density for PT2 in the resulting quartet high spin state

8. CONCLUSIONS

This TFG has explored the enhancement of the intramolecular FM coupling of BTBN by proposing 21 modified BTBN-like molecules. The idea behind all proposals was to trigger the sign of the magnetic exchange coupling in BTBN-based compounds by means of the spin polarisation SP mechanism. Spin density distributions for the studied molecules reveal the existence of spin-polarised regions, *sine qua non* condition for channelling the through-bond magnetic-exchange interactions between radical moieties. If the magnetic coupling is FM, there will be larger spin polarisation along the coupler unit in the high spin state, which will become the ground state of the BTBN-based proposal. Contrary, an AFM interaction will be the outcome of larger spin polarisation along the linker in a low spin ground state. Then, the spin polarisation mechanism enables the cooperative effect between moieties.

Specifically, after analysing all the 22 structures studied, the following conclusions can be drawn:

- For BTBN, the values of the magnetic-exchange coupling $J_{N,BTBN}$ = 56.4 cm^{-1} , and $J_{Y,BTBN}$ = 95.5 cm^{-1} have been predicted.
- The structure PA4C1D1 exhibits an enhanced FM coupling with respect BTBN. This is the reason why this A4 is established as a suitable candidate to present magnetoresistance owing to the similarities with TTF in BTBN. This A4 can also be considered as a new building block in the molecular organic magnets design.
- The use of the ethylene C2 and the azo C4 couplers connecting TTF and NN radicals results in a notorious increment of the J value for the respective PA1C2D1 and PA1C4D1 diradicals.
- The addition in the coupler structure of hydroxyl groups provides an extra coupling channel between radical moieties, increasing even more the magnetic coupling predicted, as seen for the proposals PA1C7D1-PA1C9D1.

- The radical D6 NN-Pz results to display a strong AFM behaviour, which was observed in other works for this unit in coordination compounds or metal organic frameworks.
- None of the D-type radicals designed (namely, o-verdazyl, DTDA and its Se-analogue) shows FM coupling with the TTF A1-type radical using benzene as coupler. Other structures for the coupler, such as ethylene C2, C=N in C3 and azo in C4, could be considered in future works aiming at a FM effect.
- The maximum enhancement predicted for diradical molecules is given for the structure PE1 ($J_{N,PE1} = 5.2 \bullet J_{N,BTBN}$ and $J_{Y,PE1} = 5.9 \bullet J_{Y,BTBN}$) where the ethylene and hydroxyl groups have been combined in order to induce this optimisation.
- At the light of the values of $J_{Y,TTF\text{-}NN}$, it is clear that these two triradicals (PT1 and PT2) also are promising candidates for spintronics applications.

It must be finally mentioned that predicted values of J magnetic coupling obtained using either Noodleman's or Yamaguchi's expressions show an important magnitude difference. It can be partially reasoned due to the drastic approximation applied to obtain the value of the S_{ab} overlap between *a* and *b* SOMOs in Noodleman's solution, which becomes a binary variable. Specific overlap calculation (Eq. 25) for each proposal could be solved in order to be more accurate in the predicted value, but it would not correct the inherent spin contamination. In fact, J_N can be envisaged as a lower bound and J_Y as a higher bound to the true J magnetic coupling value. Therefore, despite this difference, the conclusions extracted from all proposals prevail as valid.

9. REFERENCES AND NOTES

1. M. Kinoshita, P. Turek, M. Tamura, K. Nozawa, D. Shiomi, Y. Nakazawa, M. Ishikawa, M. Takahashi, K. Awaga, T. Inabe, Y. Maruyama, An Organic Radical Ferromagnet,,Chem. Lett. 1991, 20, 1225
2. (a) M.M. Matsushita, H. Kawakami, Y. Kawada, T. Sugawara, Negative Magneto-resistance Observed on an Ion-radical Salt of a TTF-based Spin-polarized Donor, Chem. Lett. 2007, 110. (b) M.M. Matsushita, H. Kawakami, T. Sugawara, M. Ogata, Molecule-based system with coexisting conductivity and magnetism and without magnetic inorganic ions, Phys. Rev. B, 2008, 77, 195208.
3. P. Hohenberg and W. Kohn, Inhomogeneous Electron Gas, Phys. Rev. 136, B864
4. I. Ratera, J. Veciana, Chem. Playing with organic radicals as building blocks for functional molecular materials, Soc. Rev. 2012, 41, 303
5. T. Sugawara, H. Komatsu, K Suzuki, Interplay between magnetism and conductivity derived from spin-polarized donor radicals, Chem. Soc. Rev. 2011, 40, 3105
6. Daniel K. W. Mok, Ralf Neumann, Nicholas C. HandyJ. Fragmentation of natural orbital occupation numbers-based diagnostic of differential multireference character in complexes with hydrogen bonds, Phys. Chem. 1996, 100,
7. Kitagawa, Y., Saito, T., & Yamaguchi, K. (2018). Approximate Spin Projection for Broken-Symmetry Method and Its Application. In (Ed.), Symmetry (Group Theory) and Mathematical Treatment in Chemistry. IntechOpen.
8. Louis Noodleman, Valence bond description of antiferromagnetic coupling in transition metal dimers, J. Chem. Phys. 74, 5737 (1981)
9. Iqbal A. Latif, Ved Prakash Singh, Ujjal Bhattacharjee, Anirban Panda, Sambhu N. Datta, Very Strongly Ferromagnetically Coupled Diradicals from Mixed Radical Centers. Nitronyl Nitroxide Coupled to Tetrathiafulvalene via Spacers, J. Phys. Chem. A 2010, 114, 24, 6648–6656
10. a) Avogadro: an open-source molecular builder and visualization tool. Version 1.2.0.b) Hanwell, M.D., Curtis, D.E., Lonie, D.C. et al. Avogadro: an advanced semantic chemical editor, visualization, and analysis platform. J Cheminform 4, 17 (2012).
11. A. K. Rappe, C. J. Casewit and K. S. Colwell et al, UFF, a full periodic table force field for molecular mechanics and molecular dynamics simulations. J. Am. Chem. Soc. Vol. 114(25):10024-10035.
12. Gaussian 09, Revision B.01, M. J. Frisch, G. W. Trucks, H. B. Schlegel, G. E. Scuseria, M. A. Robb, J. R. Cheeseman, G. Scalmani, V. Barone, G. A. Petersson, H. Nakatsuji, X. Li, M. Caricato, A. Marenich, J. Bloino, B. G. Janesko, R. Gomperts, B. Mennucci, H. P. Hratchian, J. V. Ortiz, A. F. Izmaylov, J. L. Sonnenberg, D. Williams-Young, F. Ding, F. Lipparini, F. Egidi, J. Goings, B. Peng, A. Petrone, T. Henderson, D. Ranasinghe, V. G. Zakrzewski, J. Gao, N. Rega, G. Zheng, W. Liang, M. Hada, M. Ehara, K. Toyota, R. Fukuda, J. Hasegawa, M. Ishida, T. Nakajima, Y. Honda, O. Kitao, H. Nakai, T. Vreven, K. Throssell, J. A. Montgomery, Jr., J. E. Peralta, F. Ogliaro, M. Bearpark, J. J. Heyd, E. Brothers, K. N. Kudin, V. N. Staroverov, T. Keith, R. Kobayashi, J. Normand, K. Raghavachari, A. Rendell, J. C. Burant, S. S. Iyengar, J. Tomasi, M. Cossi, J. M. Millam, M. Klene, C. Adamo, R. Cammi, J. W. Ochterski, R. L. Martin, K. Morokuma, O. Farkas, J. B. Foresman, and D. J. Fox, Gaussian, Inc., Wallingford CT, 2016.
13. Chemcraft - graphical software for visualization of quantum chemistry computations. https://www.chemcraftprog.com

14. Hitoshi Miyasaka* Control of Charge Transfer in Donor/Acceptor Metal–Organic Frameworks Acc. Chem. Res. 2013, 46, 2, 248–257
15. H. Komatsu, M.M. Matsushita, S. Yamamura, Y. Sugawara, K. Suzuki, T. Sugawara, Influence of Magnetic Field upon the Conductance of a Unicomponent Crystal of a Tetrathiafulvalene-Based Nitronyl Nitroxide J. Am. Chem. Soc. 2010, 132, 4528
16. Nakazaki, J., Ishikawa, Y., Izuoka, A., Sugawara, T., & Kawada, Y. (2000). Preparation of isolable ion-radical salt derived from TTF-based spin-polarized donor. Chemical Physics Letters, 319(3–4).
17. Veciana, Jaume & Cirujeda, J. & Rovira, Concepcio & Molins, Elies & Novoa, Juan. (1996). Organic Ferromagnets. Hydrogen Bonded Supramolecular Magnetic Organizations Derived from Hydroxylated Phenyl ?-Nitronyl Nitroxide Radicals. Journal de Physique I. 6. 1967-1986.
18. (a) A. W. Cordes, C. D. Bryan, W. M. Davis, R. H. de Laat,,S. H. Glarum, J. D. Goddard, R. C. Haddon, R. G. Hicks, D. K. Kennepohl, R. T. Oakley, S. R. Scott and N. P. C. Westwood, J. Am. Preparation and Characterization of the Disjoint Diradical 4,4'-Bis(1,2,3,5-dithiadiazolyl) [S2N2C−CN2S2] and Its Iodine Charge Transfer Salt [$S_2N_2C-CN_2S_2$], Chem. Soc., 1993, 115, 7232; (b) J. Campbell, D. Klapstein, P. F. Bernath, W. M. Davis, R. T. Oakley and J. D. Goddard, Experimental and Computational Evidence for "Double Pancake Bonds": The Role of Dispersion-Corrected DFT Methods in Strongly Dimerized 5-Aryl-1λ2,3λ2-dithia-2,4,6-triazines, J. Am. Chem. Soc., 1996, 35, 4264.
19. (a) P. J. Alonso, G. Antorrena, J. I. Martínez, J. J. Novoa, F. Palacio, J. M. Rawson and J. N. B. Smith, Synthesis and Magnetic Properties of the Novel Dithiadiazolyl Radical, p-$NCC_6F_4C_6F_4CNSSN$, Appl. Magn. Reson, 2001, 20, 231; (b) J. M. Rawson, C. S. Clarke and D. W. Bruce, EPR studies of the dynamics and phase behaviour of dithiadiazolyl radicals derived from mesogenic precursors, Mag n. Reson. Chem., 2009, 47,3;(c) J. Luzon, J. Campo, F. Palacio, G. J. McIntyre, J. M. Rawson, R. J. Less, C. M. Pask, A. Alberola, R. D. Farley, D. M. Murphy and A. E. Goeta, Phys. Rev. B: Condens. Spin density studies on p-O_{2}NC_{6}F_{4}CNSSN : A heavy p -block organic ferromagnet, Matter Mater. Phys., 2010, 81, 144429; (d) J. Luzón, J. Campo, F. Palacio, G. J. McIntyre, A. E. Goeta, E. Ressouche, C. M. Pask andJ. M. Rawson, Thiazyl radicals: Old materials for new molecular devices, Phys. B, 2003, 335, 1.
20. Constantinides, Christos & Eisler, Dana & Alberola, Antonio & Richards, Emma & Murphy, Damien & Rawson, Jeremy. (2014). Weakening of the π*-π* Dimerisation in 1,2,3,5-dithiadiazolyl radicals: Structural, EPR, magnetic and computational studies of dichlorophenyl dithiadiazolyls, $Cl_2C_6H_3CNSSN$. CrystEngComm. 16. 7298.
21. Nans, Roques & Gerbier, Philippe & Teki, Yoshio & Choua, Sylvie & Lesniaková, Petra & Sutter, Jean-Pascal & Guionneau, Philippe & Guérin, Christian. (2006). Towards a Better Understanding of Photo-excited Spin Alignment Processes Using Silole Diradicals, New Journal of Chemistry. 30
22. (a) A. W. Cordes, R. C. Haddon and R. T. Oakley, Phosphorus, Sulfur Silicon Relat. Elem., 2004, 179,673. (b) 13 R. C. Haddon, Design of organic metals and superconductors, Nature, 1975, 256, 394.
23. Venneri, Shari & Wilson, Justin & Rawson, Jeremy & Pilkington, Melanie. (2015). Structural, Magnetic and DFT studies on a Charge Transfer Salt of a TTF-pyridyl-(1,5-diisopropyl)verdazyl Diradical Cation. ChemPlusChem. 80.
24. Polo, Victor & Alberola, Antonio & Andres, Juan & Anthony, Jennifer & Pilkington, Melanie. (2008). Towards understanding of magnetic interactions within a series of tetrathiafulvalene-π conjugated-verdazyl diradical cation system: A density functional theory study. Physical chemistry chemical physics: PCCP. 10. 857-64.
25. Tretyakov, Evgeny & Tolstikov, Svyatoslav & Gorelik, Elena & Fedin, Matvey & Romanenko, Galina & Bogomyakov, Artem & Ovcharenko, Victor. (2008). Copper (II) complexes with pyrazolyl-substituted nitronyl and imino nitroxides. Polyhedron. 27. 739-749.
26. https://gaussian.com/dft/ , hybrid functionals, Last updated on: 30 August 2022. [G16 Rev. C.

10. ACRONYMS

TTF: Tetrathiofulvalene
NN: Nitronyl nitroxide
BTBN: di-brominated benzotetrathiofulvalene nitronyl nitroxide
FM/AFM : Ferromagnetism/Antiferromagnetism
SOMO: Sinlgy occupied molecular orbital
PES: Potential energy Surface
HF: Hartree-Fock
KS: Kohn-Sham
HK: Hohenberg-Kohn
CI: Configuration Interaction
MP: Moller-Plesset
BS: Broken Symmetry
DFT: Density Functional Theory
LCAO: Linear combination of atomic orbitals
LDA: Local density approximation
GGA: Generalized gradient approximation
LSD: Localised spin density
MV: Mixed valence
J_{AB}: Magnetic exchange coupling between A, B radicals
S_{ab}: Overlap integral between a, b orbitals
J_N: Noodleman magnetic coupling
J_Y: Yamaguchi magnetic coupling
GTO: Gaussian type orbitals